Investigation of the Thermal Stability of $Nd_xSc_yZr_{1-x-y}O_{2-\delta}$ Inert Matrix Fuel Materials

J.R. Hayes[1], M. Saoudi[2] and A.P. Grosvenor[1]
[1] University of Saskatchewan, Saskatoon, Saskatchewan, Canada
(john.hayes@usask.ca)
[2] Canadian Nuclear Laboratories (Formerly Atomic Energy of Canada Limited), Chalk River, Ontario, Canada

A PhD Level Submission

Summary

The structure and thermal stability of a series of $Nd_xSc_yZr_{1-x-y}O_{2-\delta}$ inert matrix fuel materials have been studied. The materials were analyzed using powder X-ray diffraction and X-ray absorption spectroscopy. This approach allows for an analysis of both the long-range and local structures in these materials. The results showed that the ternary $Nd_xZr_{1-x}O_{2-\delta}$ and $Sc_yZr_{1-y}O_{2-\delta}$ materials were not stable when annealed at 1400 °C, and that the quaternary $Nd_xSc_yZr_{1-x-y}O_{2-\delta}$ materials were stable when annealed if $y \geq 0.10$. This study shows that these materials may be sensitive to changes in composition, and this should be accounted for when considering the suitability of the $Nd_xSc_yZr_{1-x-y}O_{2-\delta}$ materials for inert matrix fuel applications.

1. Introduction

Developing inert matrix fuels (IMFs), which consist of transuranic elements (TRUs; i.e., Pu, Am, Np, Cm) in a neutron transparent (inert) matrix, is an important step in closing the nuclear fuel cycle [1]. Yttria-stablized cubic zirconia has been widely investigated for use as an IMF due to the chemical stability of the cubic zirconia structure, but its low thermal conductivity limits its usefulness as a nuclear fuel [2,3]. The cubic zirconia structure can be stabilized by a number of other dopants, and it is expected that adding lighter elements would improve the thermal conductivity of the material [4]. Here, the structure and thermal stability of a series of $Nd_xSc_yZr_{1-x-y}O_{2-\delta}$ materials have been studied (Nd was used a surrogate for Am). The materials were annealed at 1100 °C and 1400 °C and characterized by powder X-ray diffraction (XRD) and X-ray absorption spectroscopy (XAS). This approach allowed for an understanding of how the long-range and local structures of these materials were affected by changes in composition and annealing temperature. The results indicate that interactions between the Nd and Sc atoms may be responsible for stabilizing the cubic structure and provide important insights into the viability of $Nd_xSc_yZr_{1-x-y}O_{2-\delta}$ for use as an IMF material.

2. Experimental

2.1 Preparation of $Nd_xSc_yZr_{1-x-y}O_{2-\delta}$ Materials

The $Nd_xSc_yZr_{1-x-y}O_{2-\delta}$ materials were prepared via a co-precipitation method. Stoichiometric amounts of Nd_2O_3 and Sc_2O_3 were dissolved in boiling nitric acid and $ZrOCl_2 \cdot 8H_2O$ was separately dissolved in

~15 mL of distilled water. The acidic Nd-Sc solution was then added to the aqueous Zr^{4+} solution. Concentrated ammonia was added which resulted in the formation of a white precipitate, and the solid was collected via vacuum filtration. The materials were then calcined at 800 °C for 24 h, resulting in the final product. The thermal stability of the materials was investigated by annealing ~0.07 g aliquots of the as-synthesized material at 1100 °C and 1400 °C for 24 h.

The phase purity of the as-synthesized and annealed materials was determined by powder XRD. The powder XRD patterns were collected using a PANalytical Empyrean diffractometer equipped with a Co X-ray source. Phase quantification was obtained by Rietveld refinement which was performed using the PANalytical X'pert HighScore Plus software.

2.2 Zr K-edge X-ray Absorption Spectroscopy

Zr K-edge XAS spectra of the as-synthesized and annealed samples were collected using Pacific Northwest Consortium/X-ray Sciences Division Collaborative Access Team (PNC/XSD-CAT, Sector 20) bending magnet beamline (20BM) located at the Advanced Photon Source (APS), Argonne National Laboratory. A silicon (111) double crystal monochromator with a Rh harmonic rejection mirror was used, which has a resolution of 2.5 eV at 18000 eV and a photon flux of ~10^{11} photons/s [5]. The samples were finely ground and sealed between layers of Kapton tape, and the number of layers was adjusted to maximize the absorption signal. The Zr K-edge XAS spectra were collected in transmission mode using ion chambers filled with an Ar/N_2 gas mixture. The spectra were calibrated using a Zr metal foil, having a known Zr K-edge absorption energy of 17998 eV, and the metal foil spectrum was measured in-line with the samples [6]. The X-ray absorption near-edge (XANES) region of the Zr K-edge spectra were measured using a 0.3 eV step through the absorption edge and the extended X-ray absorption fine structure (EXAFS) region of the Zr K-edge spectra was measured to $k = 15$ Å^{-1}. All spectra were normalized and analyzed using the Demeter software suite [7].

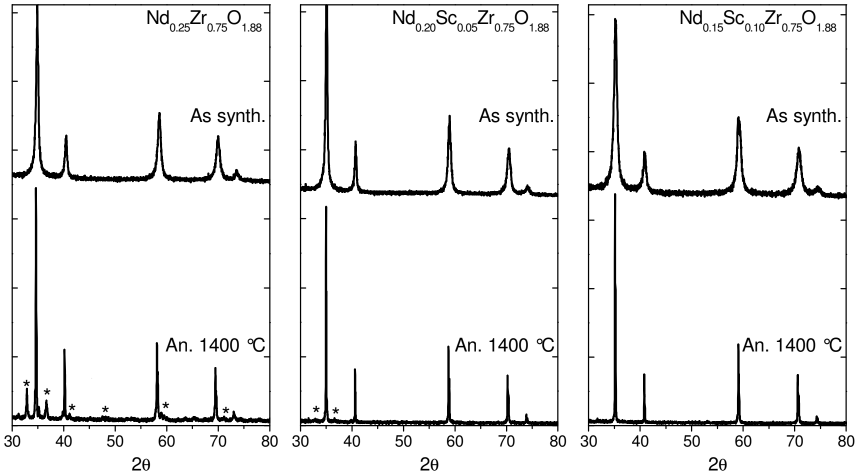

Figure 1. The powder XRD patterns from the as-synthesized and annealed (An.) (a) $Nd_{0.25}Zr_{0.75}O_{1.88}$ (b) $Nd_{0.20}Sc_{0.05}Zr_{0.75}O_{1.88}$, and (c) $Nd_{0.15}Sc_{0.10}Zr_{0.75}O_{1.88}$ materials. Peaks associated with the monoclinic phase (denoted with "*") are observed when materials with $y < 0.10$ are annealed at 1400 °C.

3. Results and Discussion

3.1 Powder X-ray Diffraction

The powder XRD patterns from several of the as-synthesized and annealed materials are presented in Figure 1. The ternary $Nd_xZr_{1-x}O_{2-\delta}$ (Figure 1a) materials partially decomposed into the lower symmetry monoclinic phase ZrO_2 when annealed at 1400 °C. This is consistent with previous results in which the materials were synthesized via a solid-state synthetic route, though the extent of decomposition was greater in the samples studied here [2]. The $Sc_yZr_{1-y}O_{2-\delta}$ materials also partially decomposed into a lower symmetry phase when annealed (not shown), though in this case a poorly understood rhombahedral Sc-Zr oxide was observed instead of the monoclinic ZrO_2 phase [8].

The stability of the fluorite structure increased as Nd was replaced by Sc in the system. Monoclinic phase ZrO_2 is still observed at low Sc content when the material was annealed, but in a much smaller quantity than in the ternary material (Figure 1b). No monoclinic phase was observed in the annealed $Nd_{0.15}Sc_{0.10}Zr_{0.75}O_{1.88}$. The results of a previous study of the $Nd_xY_yZr_{1-x-y}O_{2-\delta}$ materials indicate that the fluorite phase was stabilized when Y content was greater than or equal to 0.05 [2]. The current study shows that the cubic phase stabilization was achieved for Sc content greater than or equal to 0.10. This observation suggests that Sc^{3+} is not as effective in stabilizing the fluorite structure as Y^{3+} [2]. These results indicate that both Sc^{3+} and Nd^{3+} are required to stabilize the fluorite structure, though the nature of this stabilizing effect has not been elucidated.

3.2 Zr K-edge XAS

3.2.1 XANES

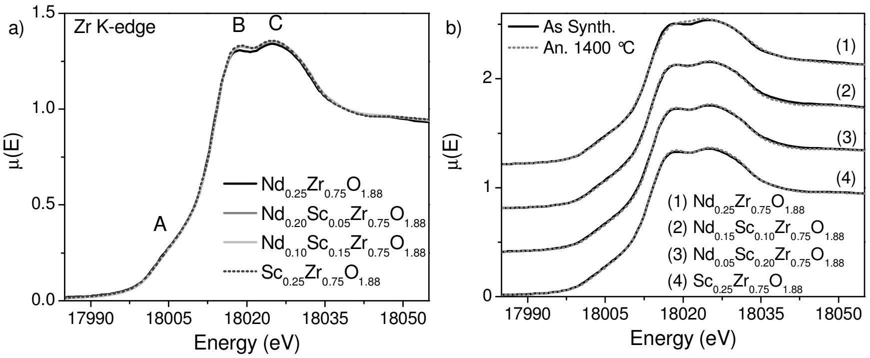

Figure 2. (a) The Zr K-edge XANES spectra from the as-synthesized $Nd_xSc_yZr_{1-x-y}O_{2-\delta}$ materials. Three features, A, B, and C are observed in the spectra. (b) The Zr K-edge spectra from the as-synthesized and annealed materials are compared. Only the spectrum from the ternary $Nd_{0.25}Zr_{0.75}O_{1.88}$ species changes upon annealing.

The Zr K-edge XANES spectra were collected and are presented in Figure 2. Three features were observed in these spectra, and are labelled A, B and C in Figure 2a. Feature A is attributed to forbidden, quadrapolar excitations of Zr 1s electrons to Zr 4d states, and features B and C are attributed to dipolar

Zr 1s → 5p transitions [2]. The intensity of Feature A did not change with composition, which indicates that the coordination geometry around the Zr centres remained relatively constant. The intensities of features B and C increased slightly as Sc replaced Nd. This change is likely caused by an increase in the Zr coordination number (CN) (see section 3.2.2). Increasing the CN would increase the number of unoccupied 5p states. The increase in unoccupied 5p states would result in the increased intensity of the 1s → 5p transitions

The Zr K-edge XANES spectra from the as-synthesized and annealed materials are presented in Figure 2b. Changes were only observed between the spectra from the as-synthesized and annealed $Nd_{0.25}Zr_{0.75}O_{1.88}$ materials, consistent with the XRD results. In this case, the energy separation between features B and C decreases and the intensity of the spectrum at ~18020 eV increases. These changes have been previously shown to be a result of a transition to a lower symmetry crystal phase [2]. No changes in the spectra were observed when the $Nd_xSc_yZr_{1-x-y}O_{2-\delta}$ materials were annealed at temperatures up to and including 1400 °C.

3.2.2 EXAFS

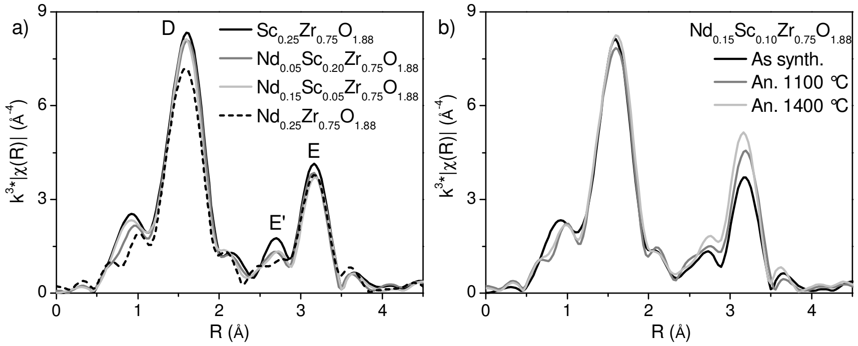

Figure 3. (a) The Fourier transform of the Zr K-edge EXAFS spectra from several of the as-synthesized $Nd_xSc_yZr_{1-x-y}O_{2-\delta}$ materials. (b) The Zr K-edge EXAFS spectra from the as-synthesized and annealed $Nd_{0.15}Sc_{0.10}Zr_{0.75}O_{1.88}$ materials are compared.

The Fourier transformed EXAFS spectra from the $Nd_xSc_yZr_{1-x-y}O_{2-\delta}$ materials are presented in Figure 3. Three features, labelled as D, E, and E' in Figure 3a, were observed in these spectra. Feature D resulted from the first coordination shell Zr–O scattering paths and the intensity increased significantly when Sc was present in the materials. This likely indicated that the addition of Sc resulted in an increased Zr CN. Feature E contains contributions from the Zr–Zr, Zr–Sc, and Zr–Nd paths while feature E' is attributed only to the Zr–Sc scattering path. There is negligible change in the intensity of feature E while the intensity of feature E' increases with increasing Sc content. This is increase in intensity is explained by the increased number of Zr–Sc paths. Fitting of the spectra indicates that the average Zr–O bond length was 2.15(1) Å and the average Zr – Zr bond length was 3.55(2) Å in all of the materials, which is consistent with the values reported for $Nd_xY_yZr_{1-x-y}O_{2-\delta}$ materials [2]. The Zr–Sc bond length determined to be 3.57(4) Å in all the as-synthesized materials. However, when the $Nd_{0.15}Sc_{0.10}Zr_{1-x-y}O_{2-\delta}$ material was annealed at 1400 °C this bond length contracted to 3.52(4) Å. (No contraction was observed when the other $Nd_xSc_yZr_{1-x-y}O_{2-\delta}$ materials were annealed at 1400 °C.)

When the $Nd_{0.15}Sc_{0.10}Zr_{0.75}O_{1.88}$ material was annealed (Figure 3b), the intensities of features E and E' were observed to increase. These increases is explained by an increase in the long-range order of the system which leads to more ordered scattering pathways. Increased ordering was observed in the powder XRD patterns as the peak widths significantly decreased when the materials were annealed at higher temperatures (see Figure 1). An analysis of the EXAFS spectra by modelling also indicates that the increase in the intensity of Peak E' may be caused by an increase in the number of Zr–Sc paths and a decrease in the number of Zr–Nd paths. This implies that Sc is preferentially occupying the Zr next-nearest-neighbour sites over Nd.

4. Conclusions

Several $Nd_xSc_yZr_{1-x-y}O_{2-\delta}$ materials were synthesized and the thermal stability of these materials was studied by annealing them at high temperatures. The powder XRD results indicated that when the materials were annealed at 1400 °C the fluorite structure was only stable in the quaternary materials if $y \geq 0.10$. The Zr K-edge XANES spectra showed that only the spectra from the $Nd_{0.25}Zr_{0.75}O_{1.88}$ changed when annealed at 1400 °C, and these changes were consistent with a transformation to a lower symmetry ZrO_2 phase. The Zr K-edge EXAFS spectra showed that the Zr coordination number likely increased with increasing Sc content and that the materials became more ordered upon annealing. These results suggest that the Sc and Nd act together to stabilize the fluorite structure and that changes in composition during in-reactor service should be accounted for when considering these materials for IMF applications. Future ion bombardment studies will be performed on these materials to understand how composition affects the material's resistance to radiation damage.

5. References

[1] C. Degueldre, J.M. Paratte "Concepts of an inert matrix fuel, an overview." *J. Nucl. Mater.* Vol. 274, Iss. 1-2, 1999, pp. 1-6.

[2] J.R. Hayes, M. Saoudi, A.P. Grosvenor "An investigation of the thermal stability of $Nd_xY_yZr_{1-x-y}O_{2-\delta}$ inert matrix fuel materials." *J. Alloys Compd.* Vol. 635, 2015, pp. 245-255.

[3] C. Ronchi, J.P. Ottaviani, C. Degueldre, R. Calabrese "Thermophysical properties of inert matrix fuels for actinide transmutation." *J. Nucl. Mater.* Vol. 320, Iss. 1-2, 2003, pp. 54-65.

[4] R.W. Keyes "High-Temperature Thermal Conductivity of Insulating Crystals: Relationship to the Melting Point." *Phys. Rev.* Vol. 115, Iss. 3, 1959, pp. 564-567.

[5] S.M. Heald, D.L. Brewe, E.A. Stern, K.H. Kim, F.C. Brown, D.T. Jiang, E.D. Crozier, R.A. Gordon, "XAFS and micro-XAFS at the PNC-CAT beamlines." *J. Synchrotron Rad.* Vol. 6, Iss. 3, 1999, pp. 347-349.

[6] A. Thompson, D. Attwood, E. Gullikson, M. Howells, K.-J. Kim, J. Kirz, J. Kortright, I. Lindau, P. Pianetta, A. Robinson, J. Scofield, J. Underwood, D. Vaughn, G. Williams, H. Winick, *X-Ray Data Booklet*; Lawrence Berkeley National Laboratory: Berkeley, 2009.

[7] B. Ravel, M. Newville "ATHENA, ARTEMIS, and HEPHAESTUS: Data Analysis for X-Ray Absorption Spectroscopy Using IFEFFIT." *J. Synchrotron Rad.* Vol. 12, Iss. 4, 2005, pp. 537–541.

[8] K. Wurst, E. Schewada, D.J.M. Bevan, J. Mohyla, K.S. Wallwork, M. Hofmann "Single-crystal structure determination of $Zr_{50}Sc_{12}O_{118}$." *Solid State Sci.* Vol. 5, Iss. 11-12, 2003, pp. 1491-1497.